

EXPERIMENTAL STUDY OF A WATER-MIST JET ISSUING NORMAL TO A HEATED FLAT PLATE

by

Andreas VOUROIS, Alexandros VOUROIS, and Thrassos PANIDIS*

Laboratory of Applied Thermodynamics, Mechanical Engineering and Aeronautics Department,
University of Patras, Patras, Greece

Original scientific paper
DOI: 10.2298/TSCI130514149V

A parametric experimental study on the development of a round jet spray impacting a smooth, heated, flat plate has been accomplished. The main objective of this effort was to provide information characterizing the flow structure of a developing mist jet, issuing vertically towards an upward facing, horizontal heated plate, by means of simultaneous droplet size and velocity measurements. Phase Doppler anemometry was used, providing also information on liquid volume flux. The fine spray of small atomized droplets (0.5-5.0 μm), was generated using a medical nebulizer. Two low Reynolds number jets ($Re = 2952$ and 3773) issuing from a cylindrical pipe have been tested. The distance between the jets exit and the plate was 50 cm. A stainless steel non-magnetic flat plate of dimensions $1000 \text{ mm} \times 500 \text{ mm} \times 12 \text{ mm}$ was used as target wall. Constant heat flux boundary conditions were established during measurements. Results indicate that the heat flux from the plate is influencing the evolution of the spray jet, diminishing its velocity and turbulence. Average droplet sizes are affected little by the heat flux, although for the non-heated sprays, droplet sizes increase at locations very close to the plate. A significant effect on droplet volume flow rate is also reported.

Key words: droplet evaporation, mist jet, phase Doppler anemometry, spray cooling

Introduction

The interaction of sprays with thermal fields and heated surfaces is of primary importance for many physical and technological applications. Droplet evaporation plays a major role in a broad class of processes, including fuel atomization in internal combustion engines and burners, fire extinguishing, atmospheric transport of rain droplets and weather forecasting. Impact jet flows are also of great interest in many industrial and technological applications, such as cooling of electronic devices, coating and drying operations, and cryogen spray cooling in laser skin treatment in dermatology.

Numerous research efforts have studied the interaction between sprays and heated surfaces, providing remarkable results and enhancing our knowledge on the heat exchange mechanisms, usually in relation to Weber number which is the most important parameter characterizing droplet behaviour [1-5]. It has been shown that higher heat transfer rates can be achieved with sprays rather than pool boiling, since the vapour removal from the surface is more efficient, and large surfaces can be cooled uniformly, with low droplet impact velocities and small temperature overshoot [6, 7]. The interaction between a spray and the buoyant plumes arising

* Corresponding author; e-mail: panidis@mech.upatras.gr

from a heated surface has been also studied, pointing out a considerable reduction in droplet velocity due to the counter flowing buoyant plumes [8]. Surface wettability and liquid physical properties such as surface tension, viscosity and effusivity, influence the spray process and particularly the spreading dynamics, and the heat transfer characteristics of the so-called *gently deposited* droplets, *i. e.* in cases with a low Weber number, $We < 5$ [9]. Single drop impact including secondary atomization effects has been studied to provide information on the main physical mechanisms which are responsible for the wall spray interaction and the characterization of the cooling regimes [9-14]. Spray cooling is indeed much more complicated, involving spray characteristics such as droplet size-velocity and number density correlations. The thermal interaction between spray droplets and vapour during pre-impact seems to have a significant influence on the heat transfer process during spray cooling [15], while it has been reported that in certain conditions dilute sprays with large velocities are more effective than low velocity dense sprays [16]. The identification of cooling regimes for sprays impacting on heated surfaces is supported by significant studies on the modifications of droplets' morphology during impact.

In this paper, a parametric study on the effect of heating on the development of a mist spray issuing normal to a heated plate is presented, based on droplet velocity and size measurements. Mist generated by a medical nebulizer was used to produce round jet sprays at two Reynolds numbers ($Re = 2952$ and 3773). The plate was either isothermal to the spray and the flow field or heated at two different heat fluxes of 1140 and 1380 W/m^2 .

Experimental facility

The spray was produced by a commercial medical air-water nebulizer. The process was controlled by a regulated air supply. The liquid was blended in the nebulizer with the incoming compressed airflow, producing atomized droplets of small size ($0.5\text{-}5 \mu\text{m}$). The fine jet spray issued from a cylindrical pipe of 40 cm length and of 4 mm inner diameter, forming a round jet, with its axis normal to the centre of a horizontal, flat, smooth heated plate. The distance between the jet exit and the surface was 50 cm . Since this distance implies a non-dimensional surface to jet exit spacing, h/d of 125 this jet cannot be categorized as impinging.

A stainless steel, non-magnetic, smooth, flat plate of dimensions $1000 \text{ mm} \times 500 \text{ mm} \times 12 \text{ mm}$ was used as target wall for the jets. Stainless steel plates have the advantage to be less sensitive to alterations of surface properties due to continuous heating, in contrast to aluminium plates. An open top cavity was formed over the plate of dimensions $1000 \text{ mm} \times 500 \text{ mm} \times 500 \text{ mm}$ with transparent glass windows as sidewalls, supported on an aluminium frame allowing optical access. The plate was heated by uniformly spaced resistor elements (Ni-Cr alloy) attached to its lower side. Temperature uniformity on the plate surface was achieved by adjusting the power supply to each element. The plate was encased flush in an insulating box minimizing heat losses from its lower surface and side edges. Hence, the heat flux from the upper surface at steady-state could be estimated directly from the electrical power consumption. Constant heat flux boundary conditions were established. A detailed description of the experimental apparatus and the induced thermal field, in the absence of a spray, has been presented elsewhere [17]. The homogeneity of the surface temperature was checked by thermocouple measurements at a depth of 1 mm from the plate surface, using blind holes drilled at the back side.

The phase Doppler anemometry (PDA) technique has been employed for simultaneous measurements of droplet size and velocity. This technique is insensitive to the amplitude of the scattered light and provides additional local point information including liquid volume flux, droplet number density, and size-velocity correlation. A 30 mW laser with 632.8 nm wavelength was used with a beam of 1 mm diameter. A beam splitter was used to produce

two parallel beams at 50 mm distance. The set-up of receiving and transmitting optics has been selected and optimized according to the measurement requirements and optical access limitations. The beams were focused at the measurement location with a lens, with 605 mm focal length, producing a control volume of 64 fringes with $7.67 \mu\text{m}$ fringe spacing. A similar lens at 30° off-axis position was used to collect the scattered light from individual particles within the measuring volume. The signal was analysed by a burst spectrum analyser (Dantec BSA 57 \times 10), based on 10% spherical validation and 10° phase error criteria. At each measuring location 20,000 validated samples were recorded. Sampling rate was depending on droplet presence and signal validation, maintaining a mean value of 800 Hz close to the spray axis. A sketch of the experimental configuration is presented in fig. 1.

Measurement uncertainty depends on the uncertainties of droplet diameter and velocity. Error analysis resulted to an uncertainty of 3% for the mean droplet size, 1% for the mean velocity, 3% for the rms velocity, and about 16% for the volume flux measurements for 95% confidence level [18]. It is commonly accepted that accurate volume flux measurements are more difficult to obtain than size or velocity measurements, whereas the magnitude of the uncertainty on flux measurements depends on the droplets size range and the optical arrangement. Moreover, the uncertainty in volumetric flux depends on the ratio of droplet-to-probe volume diameter and the probability of droplets crossing the probe volume with specific trajectories, and can be kept small if the probe volume is larger than the maximum droplet diameter in the flow [19-22].

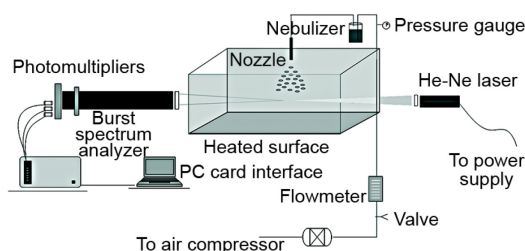


Figure 1. The experimental set-up

Results and discussion

Measurements refer to a Cartesian co-ordinate system with its origin located at the centre of the jet exit. The plate surface is parallel to the x-y plane, with the x-axis parallel to the long dimension of the plate and the z-axis pointing downwards. The jet axis is coinciding with the z-axis (fig. 1). Measurements were carried out along the axis of the jet, over the whole distance between the jet exit and the flat plate and radial profiles were measured at several locations downstream of the jet exit, according to the spreading of the jet. Since the pipe aspect ratio is large enough ($l/d = 100$), a fully developed profile of the axial mean velocity may be anticipated at jet exit.

The PDA measurements were organized: two isothermal reference test cases (A1, A2) were monitored first. The corresponding mean jet exit velocities were measured as 11.44 m/s and 14.62 m/s at a distance of $1d$ from the nozzle, implying $Re = 2952$ and 3773 , respectively. In this series of experiments the flat plate was not heated. Then the plate was heated uniformly at two power levels, establishing two different heat fluxes on the plate surface of 1140 W/m^2 (L case) and 1380 W/m^2 (H case). Each one of the reference jets (A1, A2) was studied under the influence of both heat fluxes (L, H). The characteristic conditions of all test cases are presented in tab. 1.

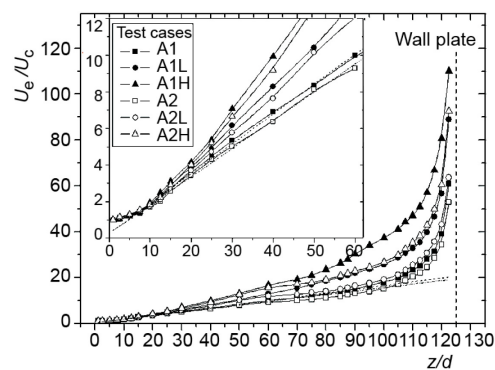
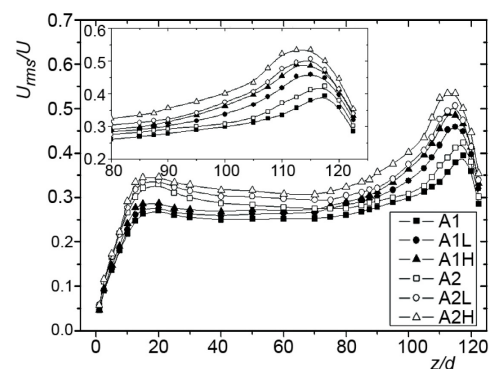
Centreline properties of spray jets

The centreline velocity, U_c , evolution in a free jet is usually presented in terms of U_c/U_c (where U_c is the jet exit velocity). In this form, a linear dependence with the distance

Table 1. Reference conditions of the test cases

Test case	Jet exit velocity [ms^{-1}]	Reynolds number	Plate surface temperature [$^{\circ}\text{C}$]	Heat flux [Wm^{-2}]
A1	11.44	2952	25	0
A1L			90.08	1140
A1H			105.05	1380
A2	14.62	3773	25	
A2L			90.08	1140
A2H			105.05	1380

ity for the isothermal jets (test cases A1, A2) presents linear distributions almost to $100 z/d$. Linear fitting curves are depicted by dashed lines. The decay constant (*i. e.* the inverse of the slope) was calculated 6.13 and 6.49 for the low and high flow rate isothermal cases, respectively (A1, A2). Farther downstream, the distributions are departing from the linear trend, indicating a reduction of the mean centreline velocity due to the influence of the flat plate. In the presence of a heating flux from the plate, the distributions diverge from those of the isothermal test cases, indicating a reduction of the centreline velocity even at axial distances in the range 15-20 z/d (a distance of more than 40 cm from the plate). This influence, also seems to undermine the linear behaviour of the inverse velocity, which is more obvious for the higher heat flux and the lower Reynolds number jet. In the far field, close to the plate, the presence of a heating flux has a significant effect on the centreline velocity, which in any case has a zero value on the plate. The buoyant plumes seem to significantly oppose the jet evolution, especially for the low Reynolds number jet.

**Figure 2. Distributions of mean axial velocity for all test cases****Figure 3. Axial distributions of droplet turbulent intensity**

of about 30% and 35% at the end of the potential core for the low and high Reynolds number jets, respectively, fluctuating values reach a plateau. Besides the effect of the Reynolds number, an effect of the heating rate is also observed in the overshoot and the plateau values,

from jet exit is observed. The jet exit velocity during each of the test cases examined remained constant within $\pm 0.5\%$. In fig. 2, non-dimensional distributions of the inverse mean axial velocity over $122.5 z/d$ are presented, whereas at the inset the same distributions over $60 z/d$ are shown. The dashed vertical line at $125 z/d$ indicates the surface of the flat plate. The axial velocity

for the isothermal jets (test cases A1, A2) presents linear distributions almost to $100 z/d$. Linear fitting curves are depicted by dashed lines. The decay constant (*i. e.* the inverse of the slope) was calculated 6.13 and 6.49 for the low and high flow rate isothermal cases, respectively (A1, A2). Farther downstream, the distributions are departing from the linear trend, indicating a reduction of the mean centreline velocity due to the influence of the flat plate. In the presence of a heating flux from the plate, the distributions diverge from those of the isothermal test cases, indicating a reduction of the centreline velocity even at axial distances in the range 15-20 z/d (a distance of more than 40 cm from the plate). This influence, also seems to undermine the linear behaviour of the inverse velocity, which is more obvious for the higher heat flux and the lower Reynolds number jet. In the far field, close to the plate, the presence of a heating flux has a significant effect on the centreline velocity, which in any case has a zero value on the plate. The buoyant plumes seem to significantly oppose the jet evolution, especially for the low Reynolds number jet.

Profiles of droplets' fluctuating velocity normalized with the centreline velocity at each downstream distance are depicted in fig. 3, where the near wall region has been enlarged at the inset. In the jet near field, the droplet velocity fluctuations increase rapidly within the potential core. The rate of increase and the peak values are larger for the high Reynolds number jet. Farther downstream, after a weak overshoot

which partially may be attributed to the corresponding differences of the centreline velocities. Close to the plate, this normalization produces high values, indicating that the centreline velocity is decreasing more rapidly with downstream distance than the fluctuations, in particular for the heating cases. This is more evident close to the plate, after about $z/d = 115$.

Corresponding information regarding the size of the droplets as the mist jets are developing downstream is presented in fig. 4. As the most appropriate metric for droplet-air mass transfer processes, the Sauter mean diameter (SMD), D_{32} , is used. This variable represents the diameter of an equivalent droplet that has the same average volume and average surface area with the droplet population of the spray [23]. In the jet (very) near field, although the droplets at jet exit have similar diameters, the diameters in the high Reynolds number jet decrease rapidly with downstream distance, unlike the droplets of the slower jet which decrease at a lower rate. This different behaviour should be probably attributed to the different shear developing in the jets. At this stage, a weak influence of the heating becomes discernible only after $z = 5-10$ cm, resulting in smaller droplet diameters, with a consistent trend, until about 10 cm from the plate. Heating has a larger impact on the droplet sizes of the low Reynolds number jet. Close to the wall, the SMD of the isothermal jet droplets increases considerably, as also do, to a lesser degree, the droplets of the high heating rate cases.

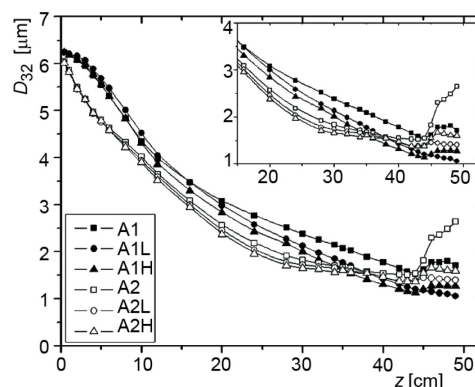
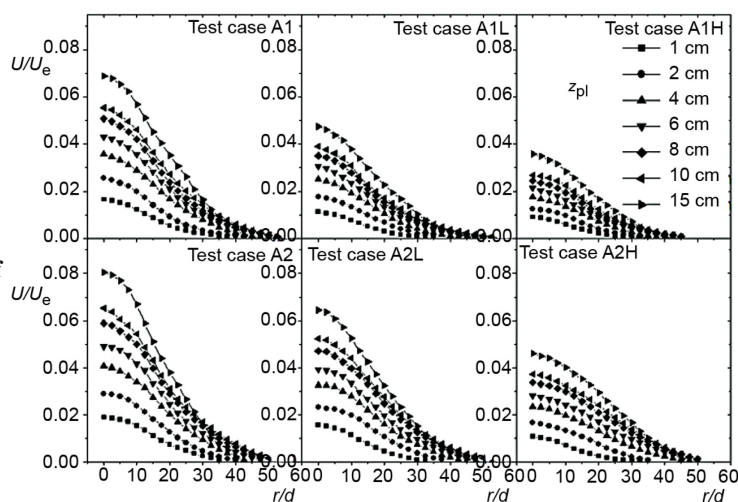


Figure 4. Spatial evolution of D_{32} for all test cases

Properties distributions close to the plate

To provide complementing information on spray behaviour close to the wall, radial profiles of the mean and rms streamwise velocity as well as the SMD of the droplets are presented in figs. 5-7. In these graphs, z_{pl} indicates the distance from the plate surface (located at $z = 50$ cm from jet exit). Measurements were accomplished to the outmost radial distances

Figure 5. Transverse profiles of droplet mean axial velocity at the near wall-plate locations



where droplets are encountered, satisfying the PDA validation criteria. The closest to the plate location was $z_{pl} = 1$ cm due to limitations of the optical path. Radial distances have been normalized by the orifice diameter of the nozzle.

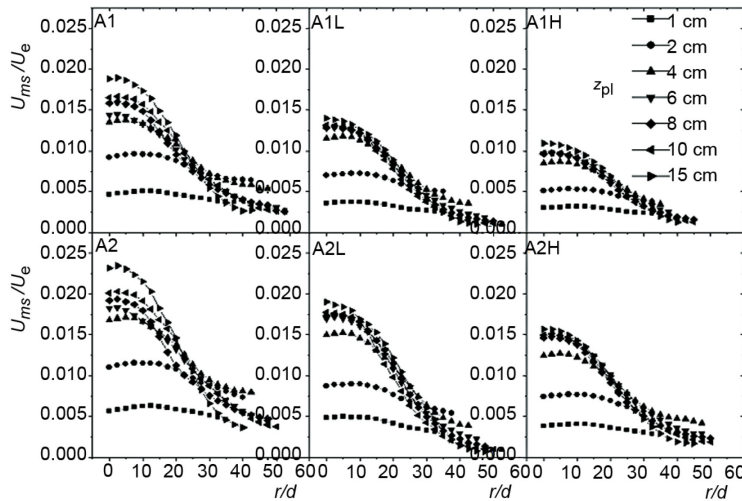


Figure 6. Transverse profiles of droplet fluctuating velocity at the near wall-plate locations

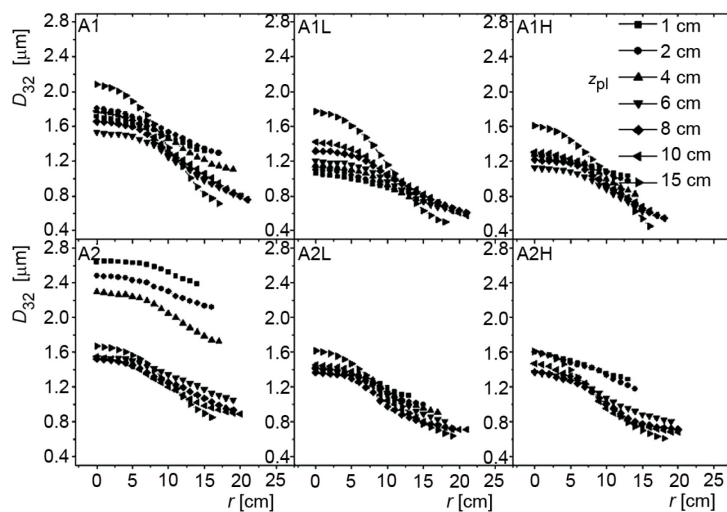


Figure 7. Transverse profiles of SMD at the near wall-plate locations

The mean droplet velocities for all test cases are presented in fig. 5. Values have been normalized by the jet exit velocity of the corresponding test cases A1, A2, since measurements showed that the plate heat flux did not affect the jet exit velocity. Far from the plate, the mean velocity distributions resemble those of a free jet, with values decreasing with distance from the jet exit whereas the extent of the jet is still increasing. Closer to the plate, the values of the mean streamwise velocities decrease further, and from a certain point, the width of the jet is also decreasing due to the stagnation on the wall. The high Reynolds number jet seems to produce a narrower jet of higher velocities. Heating seems to suppress jet velocities and results in the decrease of the radial extent of the jets.

Velocity fluctuations distributions, presented in fig. 6, illustrate the effect of the stagnation region close to the plate surface. Far from the plate, the distributions resemble

those of a free jet, extending in a similar area, with peak values close to the centreline. In the vicinity of the plate, the distributions have considerably lower values, the peak has moved farther from the centreline, and the values continue to be comparable to those at the central area until the edges of the jet. Values are in general larger for the high Reynolds number jet whereas heating seems to also suppress the fluctuations.

Radial profiles of D_{32} , SMD are presented in fig. 7. Peak values are observed at locations close to the jet axis, decreasing with the distance from the jet exit, at locations away from the plate surface. In the vicinity of the plate, for the isothermal cases, values increase again. It is interesting to note that whereas for the low heat flux cases the values are rather decreasing as the sprays approach the plate, in the high heat flux case a small increase is observed. The increase of sizes close to the plate is probably associated with the droplet-surface interaction due to rebound and splashing and the complete evaporation of the very small droplets. These small droplets when impacting the surface are highly evaporated and consequently, lead to a reduction of the average surface in a greater degree than that of the average volume [24]. This behaviour may also be affected by the dependence of surface tension on temperature. The disintegration of a droplet impacting onto a rigid surface occurs as the inertial effects unbalance capillary effects, due to opposed action between the destabilizing kinetic energy of the droplet at impact and the stabilizing surface energy maintaining the shape of the droplet [25]. Droplet disintegration is characterized by a critical impact velocity, depending on surface properties and the Weber number, $We = \rho D_0 U_0^2 / \sigma$, where ρ , σ , D_0 , and U_0 are the density, the surface tension of the liquid, the initial diameter, and the impact velocity of the droplets, respectively. Water is usually taken as a reference fluid depicting the critical Weber number for the onset of droplet water splash. As the plate is heated and increased values of the surface temperature are established, the values of droplets surface tension are decreased in comparison to the non-heated cases. Droplets of a higher surface tension liquid impacting onto a rigid surface have been found to produce less secondary droplets but with larger mean size diameters, in comparison with lower surface tension liquid droplets [25].

Flow rate considerations

Since the sprays are dilute and the droplets very small, we may assume that they closely follow the air flow as seeding particles. We may therefore estimate the air volume flow rate integrating radially the measured mean axial velocity profiles at each cross plane as described in eq. (1):

$$Q_{\text{air}} = 2\pi \int_0^r rU(r)dr \quad (1)$$

In fig. 8 the calculated air volume flow-rate at each measurement plane is presented. The evolution of the flow-rate downstream provides complementing information in relation to the centreline velocity evolution diagrams and jet spreading. Initially, all the test cases retain the character of a free jet. As the jets are leaving the nozzle, they begin to entrain the surrounding still air, resulting to increased values of air volume flow rate, at downstream cross planes and broadening the mixing zone. The distri-

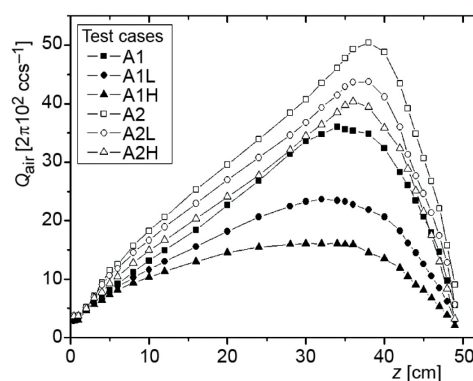


Figure 8. Distributions of calculated air volume flow-rates

butions are increasing almost linearly from jet exit to a downstream distance which depends on jet Reynolds number and heating flux. In cases involving a heat flux, especially for the low Reynolds number jet, the departure from the linear increase trend should be probably attributed to the opposing action of buoyant rising plumes, whereas at locations closer to the flat plate the volume flow-rate is diminishing, due to the presence of a stagnation point at the centre of the plate and the development of a radial flow parallel to the plate (wall jet).

Integrating radially the droplet massflux measurements obtained by the PDA, the liquid mass flow-rate can be calculated. This is presented in fig. 9 in non-dimensional form. In the near field, it can be surmised that the decrease in the flow-rate along the jet axis occurs due to the evaporation of water droplets. Close to the plate, this assumption is not accurate, since the radial flow parallel to the plate is expected to carry a fraction of the droplets outside

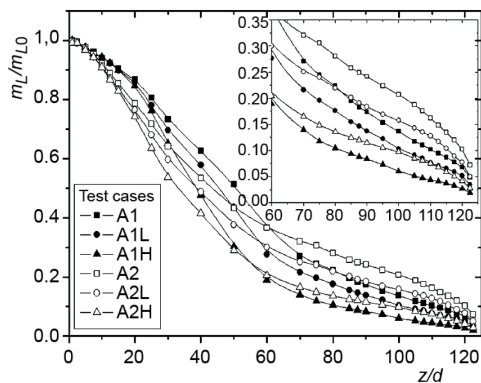


Figure 9. Distributions of calculated cross-plane droplet massflux

the measuring domain. It is interesting to observe that in the near field the evaporation of droplets is relatively more intense for the high Reynolds number jet. This may be attributed to the higher shear produced in the high Reynolds number jet establishing a higher mass transfer coefficient at the droplet surface.

The presence of a heat flux enhances the evaporation process. Further downstream, the relative evaporation in the lower Reynolds number jet increases in comparison to the high Reynolds number jet, a behaviour which may be attributed to the lower velocities and higher residence times of these jets. At the inset, the near wall region to the plate is presented for clarity. Different trends are observed depending on Reynolds number and heating. For example, at the near field and over $30 z/d$, the mass flux distributions of lower Reynolds number test cases are lying at higher levels in comparison to those of the higher Reynolds number jets. Farther downstream, they are crossing the distributions of higher Reynolds number test cases, before they rest at lower levels in the plate near wall region as compared to the same heat flux conditions. The last observation is more clearly seen after $70 z/d$.

Conclusions

A parametric experimental study on the development of round jet sprays emanating normally to a flat heated plate has been accomplished. Simultaneous droplet size and velocity measurements along with flow-rate estimations obtained with PDA have been presented. The configurations under study involved two types of spray jets of Reynolds numbers 2952 and 3773, interacting with a plate heated at two different heating rates. The isothermal case was also monitored for reference.

Streamwise distributions of velocity statistics indicate that heat flux from the plate is influencing the evolution of the spray jet, diminishing its velocity and turbulence. The increase of the heat flux results to somewhat smaller droplets at locations far from the heated plate. This trend is consistent for both jets' Reynolds numbers. Increased values of SMD are observed close to the heated plate, indicating the droplet – plate interaction due to rebound, splashing and evaporation. The heat flux has a direct impact on droplet volume flow rate evolution, while its

presence also affects the evaporation process. Mass fluxes distributions are characterized by slightly different trends, depending on Reynolds numbers and heating flux.

Nomenclature

D_{32} – droplet Sauter mean diameter, [μm]
 d, l – nozzle pipe diameter and length, respectively, [m]
 h – distance between jet exit and wall target, [m]
 m – liquid mass flow-rate, [kg s^{-1}]
 Q – volume flow-rate, [$\text{m}^3 \text{s}^{-1}$]
 Re – Reynolds number ($= Ud/\nu$), [-]
 r – radial distance from the jet centreline, [m]
 U – axial velocity, [ms^{-1}]
 We – Weber number ($= \rho D_0 U_0^2 / \sigma$), [-]
 z – vertical distance from the jet exit, [m]

z_{pl} – vertical distance from the plate, [m]

Greek symbols

ν – kinematic viscosity, [$\text{m}^2 \text{s}^{-1}$]
 ρ – density of gas, [kg m^{-3}]
 σ – liquid surface tension, [Nm^{-1}]

Subscripts

c – centreline
 e – exit
 pl – plate

References

- [1] Jia, W., Qiu, H.-H., Experimental Investigation of Droplet Dynamics and Heat Transfer in Spray Cooling, *Exp. Thermal and Fluid Science*, 27 (2003), 7, pp. 829-838
- [2] Grissom, W. M., Wierum, F. A., Liquid Spray Cooling of a Heated Surface, *Int. J. Heat Mass Transfer*, 24 (1981), 2, pp. 261-271
- [3] Qiao, Y. M., Chandra, S., Spray Cooling Enhancement by Addition of a Surfactant, *ASME J. Heat Transfer*, 120 (1998), 1, pp. 92-98
- [4] Yao, S. C., Choi, K. J., Heat Transfer Experiments of Mono-Dispersed Vertically Impacting Sprays, *Int. J. Multiphase Flow*, 13 (1987), 5, pp. 639-648
- [5] Zhang, S., Gogos, G., Film Evaporation of a Spherical Droplet over a Hot Surface: Fluid Mechanics and Heat/Mass Transfer Analysis, *J. Fluid Mechanics*, 222 (1991), Jan., pp. 543-563
- [6] Horacek, B., *et al.*, Single Nozzle Spray Cooling Heat Transfer Mechanisms, *Int. J. Heat Mass Transfer*, 48 (2005), 8, pp. 1425-1438
- [7] Lin, L., Ponnappan, R., Heat Transfer Characteristics of Spray Cooling in a Closed Loop, *Int. J. Heat Mass Transfer*, 46 (2003), 20, pp. 3737-3746
- [8] Gonzalez, J. E., Black, W. Z., Study of Droplet Sprays Prior to Impact on a Heated Horizontal Surface, *ASME J. Heat Transfer*, 119 (1997), 2, pp. 279-287
- [9] Cossali, G. E., *et al.*, Thermally Induced Secondary Drop Atomization by Single Drop Impact onto Heated Surfaces, *Int. J. Heat Fluid Flow*, 29 (2008), 1, pp. 167-177
- [10] Bernardin, J. D., *et al.*, Mapping of Impact and Heat Transfer Regimes of Water Drops Impinging on a Polished Surface, *Int. J. Heat Mass Transfer*, 40 (1997), 2, pp. 247-267
- [11] Chandra, S., Avedisian, C. T., On the Collision of a Droplet with a Solid Surface, *Proc. Royal Soc.*, 432 (1991), 1884, pp. 13-41
- [12] Chaves, H., *et al.*, Dynamic Processes Occurring During the Spreading of Thin Liquid Films Produced by Drop Impact on Hot Walls, *Int. J. Heat Fluid Flow* 20, (1999), 5, pp. 470-476
- [13] Di Marzo, M., *et al.*, Evaporative Cooling Due to a Gently Deposited Droplet, *Int. J. Heat Mass Transfer*, 36 (1993), 17, pp. 4133-4139
- [14] Ko, Y. S., Chung, S. H., An Experiment on the Break-Up of Impinging Droplets on a Hot Surface, *Exp. In Fluids*, 21 (1996), 2, pp. 118-123
- [15] Yoshida, K., *et al.*, Spray Cooling under Reduced Gravity Conditions, *ASME J. Heat Transfer*, 123 (2001), 2, pp. 309-318
- [16] Kim, J., Spray Cooling Heat Transfer: The State of the Art, *Int. J. Heat Fluid Flow*, 28 (2007), 4, pp. 753-767
- [17] Vouros, A., Panidis, Th., Statistical Analysis of Turbulent Thermal Free Convection over a Horizontal Heated Plate in an Open Top Cavity, *Exp. Thermal and Fluid Science*, 36 (2012), Jan., pp. 44-55
- [18] Tate, R. W., Some Problems Associated with the Accurate Representation of Droplet Size Distributions, *Proceedings*, 2nd International Conference on Liquid Atomic and Spray Systems, Madison, Wis., USA, 1982

- [19] Hardalupas, Y., et al., Mass Flux, Mass Fraction and Concentration of Liquid Fuel in a Swirl – Stabilized Flame, *Int. J. Multiphase Flow*, 20 (1994), Suppl., 1, pp. 233-259
- [20] Tropea, C., et al., Dual – Mode Phase – Doppler Anemometer, *Part. Particle & Particle Systems Characterization*, 13 (1996), 2, pp. 165-170
- [21] Widmann, J. F., et al., Improving Phase Doppler Volume Flux Measurements in Low Data Rate Applications, *Measurement Science and Technology*, 12 (2001), 8, pp. 1180-1190
- [22] Saffman, M. Automatic Calibration of LDA Measurement Volume Size, *Applied Optics*, 26 (1987), 13, pp. 2592-2597
- [23] Lefebvre, A. H., *Atomization and Sprays*, Taylor & Francis Hemisphere, New York, USA, 1989
- [24] Zhou, Z., et al., An Experimental Study on the Spray and Thermal Characteristics of R134a Two-Phase Flashing Spray, *Int. J. Heat Mass Transfer* 55, (2012), 15-16, pp. 4460-4468
- [25] Moita, A. S., Moreira, A. L. N., Drop Impacts onto Cold and Heated Rigid Surfaces: Morphological Comparisons, Disintegration Limits and Secondary Atomization, *Int. J. Heat Fluid Flow* 28 (2007), 4, pp. 735-752